The 188th ISIJ Meeting

Date

September 18 to 20, 2024
Reception: 8:15 - 16:00 (September 18 to 19), 8:15 - 14:00 (September 20)

Venue

Osaka University, Toyonaka Campus
Machikaneyama, Toyonaka, Osaka, Japan

Access to Osaka University

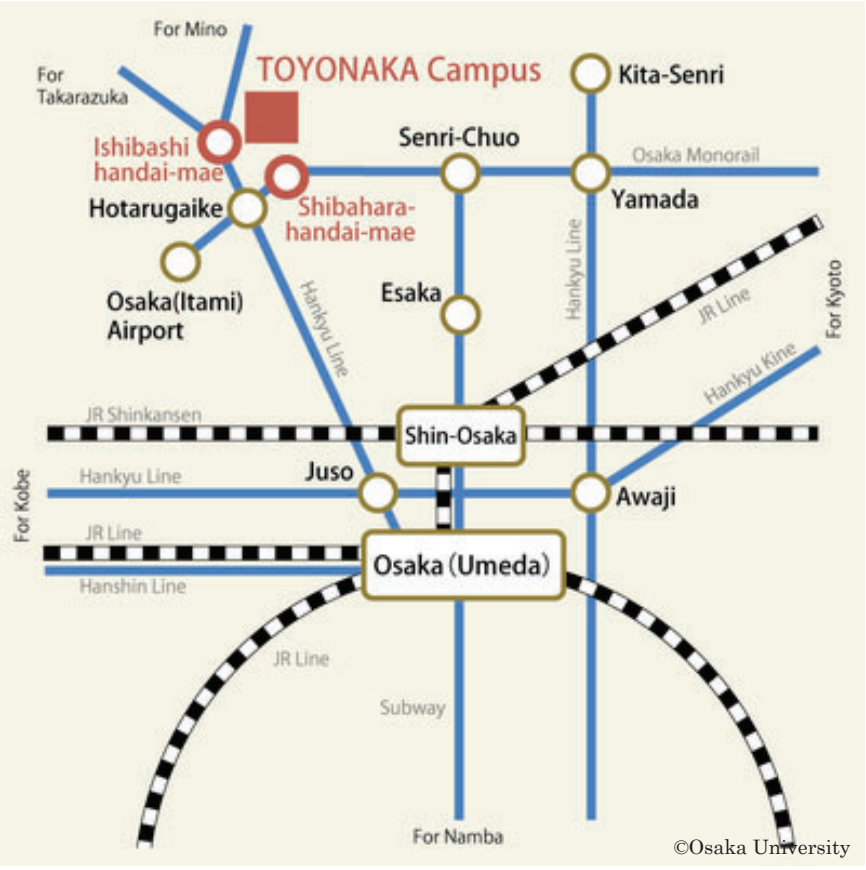

By Train:
15 min. east on foot from Ishibashi handai-mae on Hankyu Takarazuka Line.

By Monorail:
10 min. west on foot from Shibahara-handai-mae on Osaka Monorail.

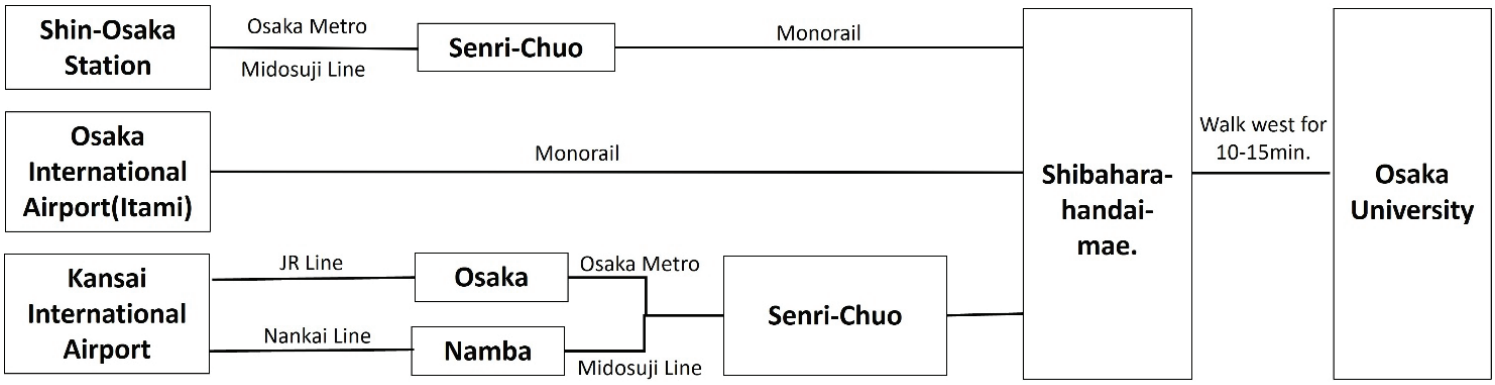

For more information, please see the following website.
https://www.osaka-u.ac.jp/en/access/top

Campus map

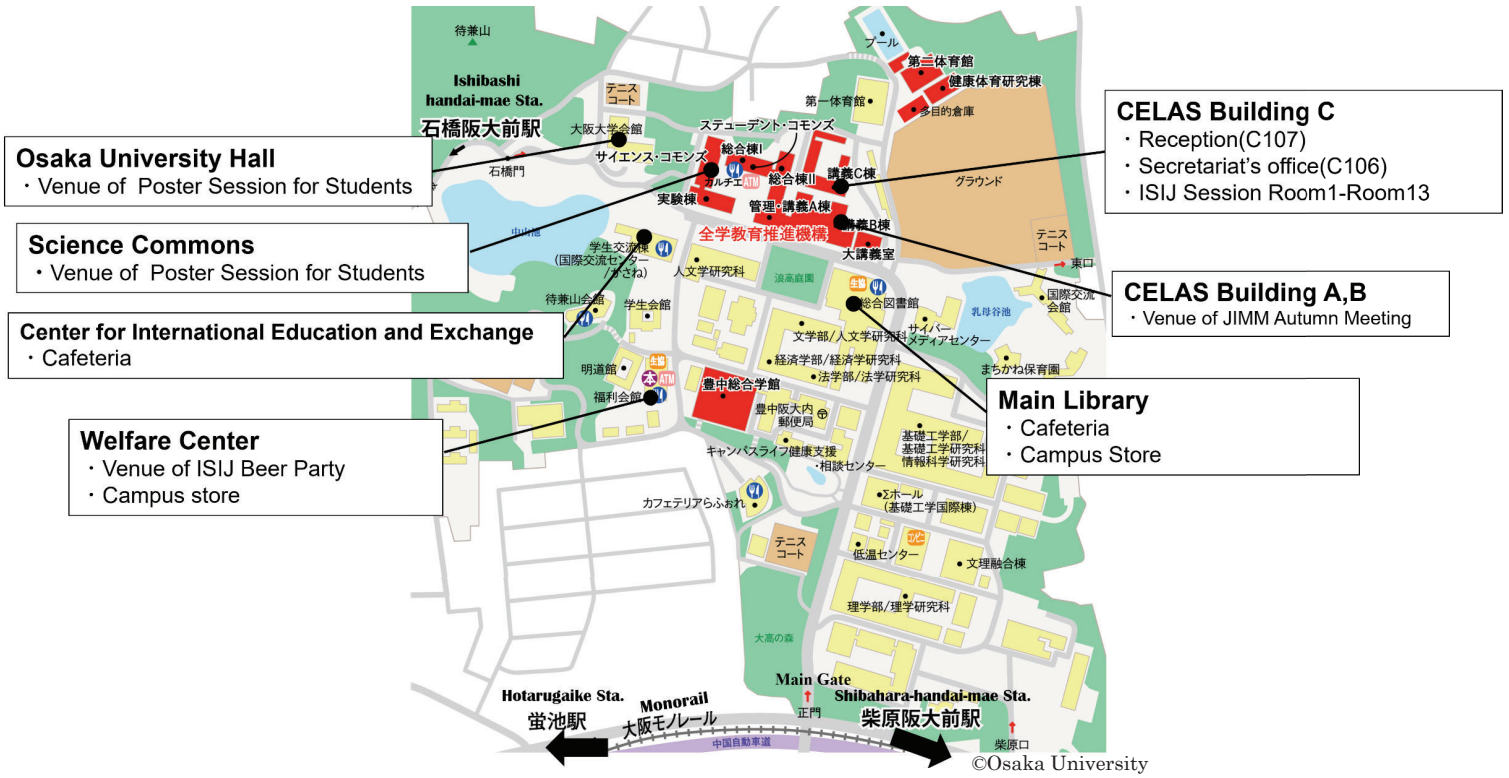

Center for Education in Liberal Arts and Sciences(CELAS)
Lecture Building C

1st Floor

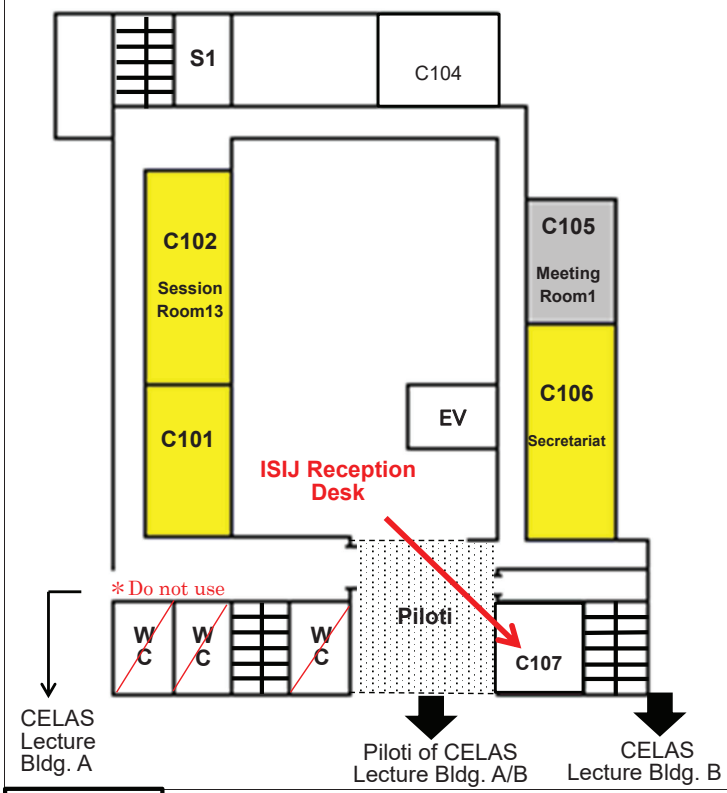

2nd Floor

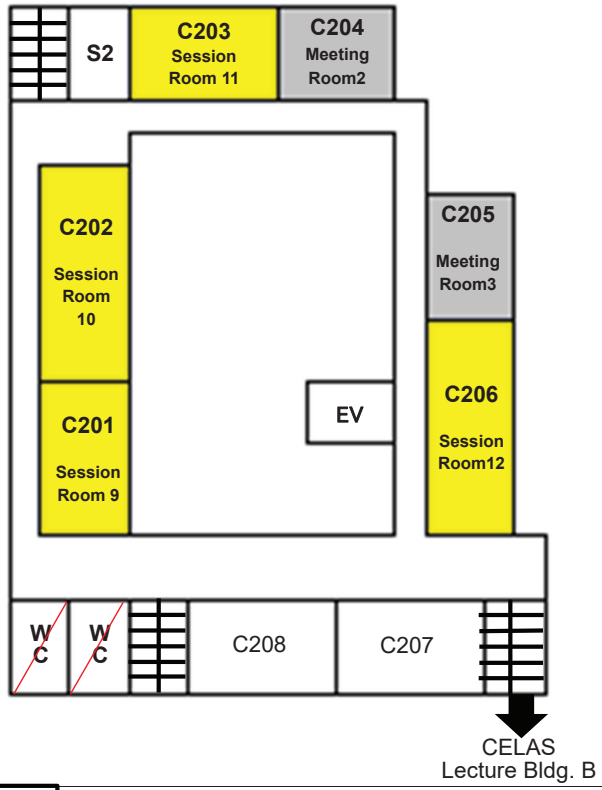

3rd Floor

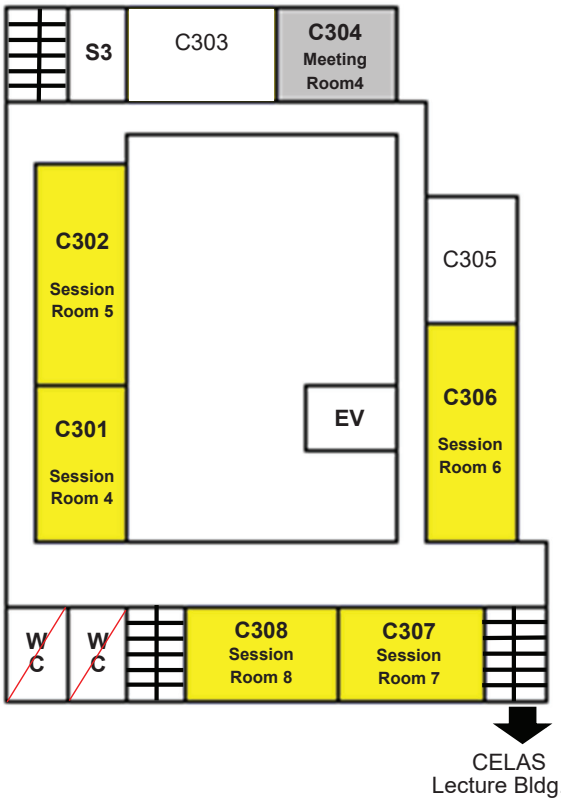

4th Floor

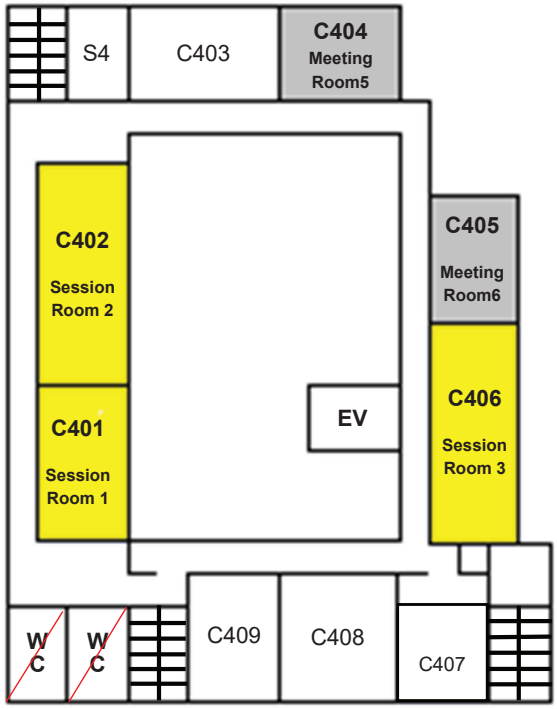

Center for Education in Liberal Arts and Sciences(CELAS)
Lecture Building A, B

1st Floor

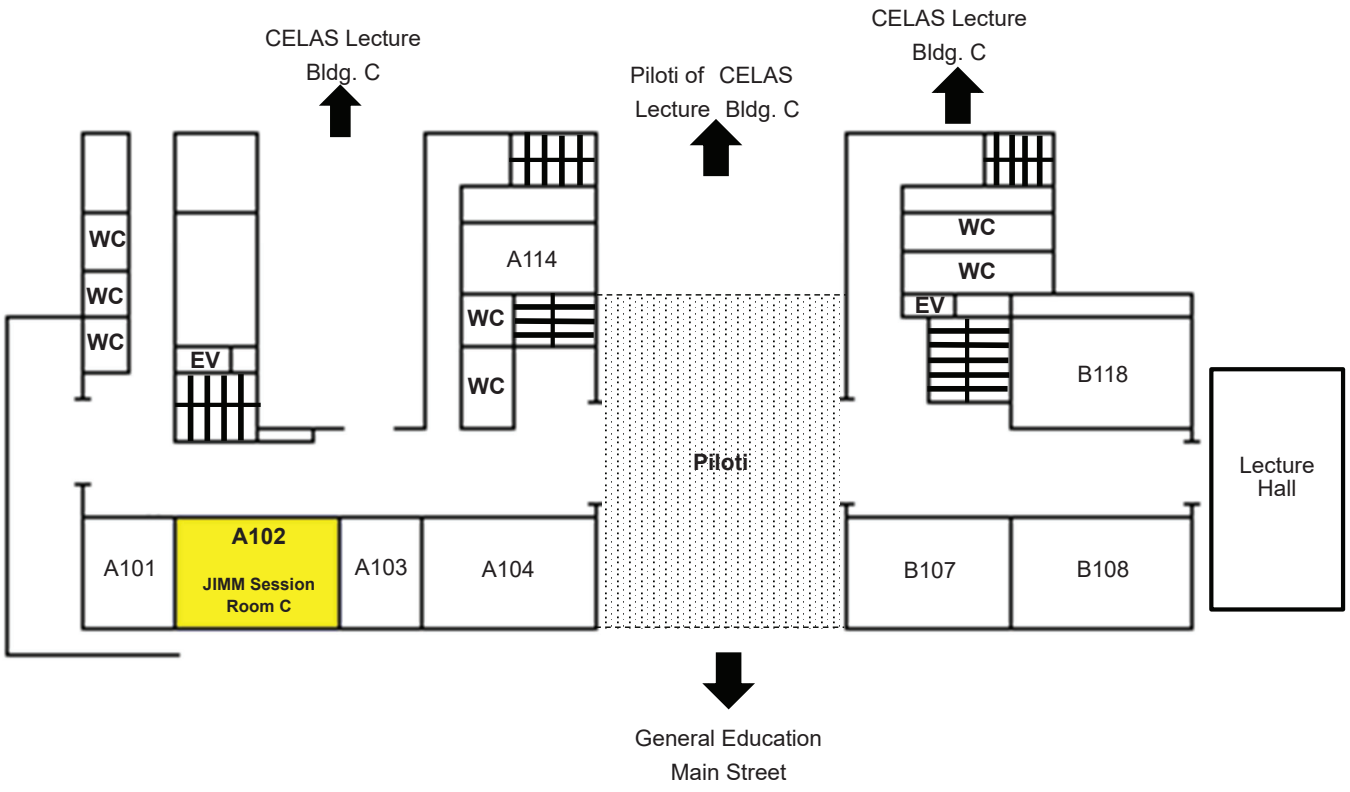

3rd Floor

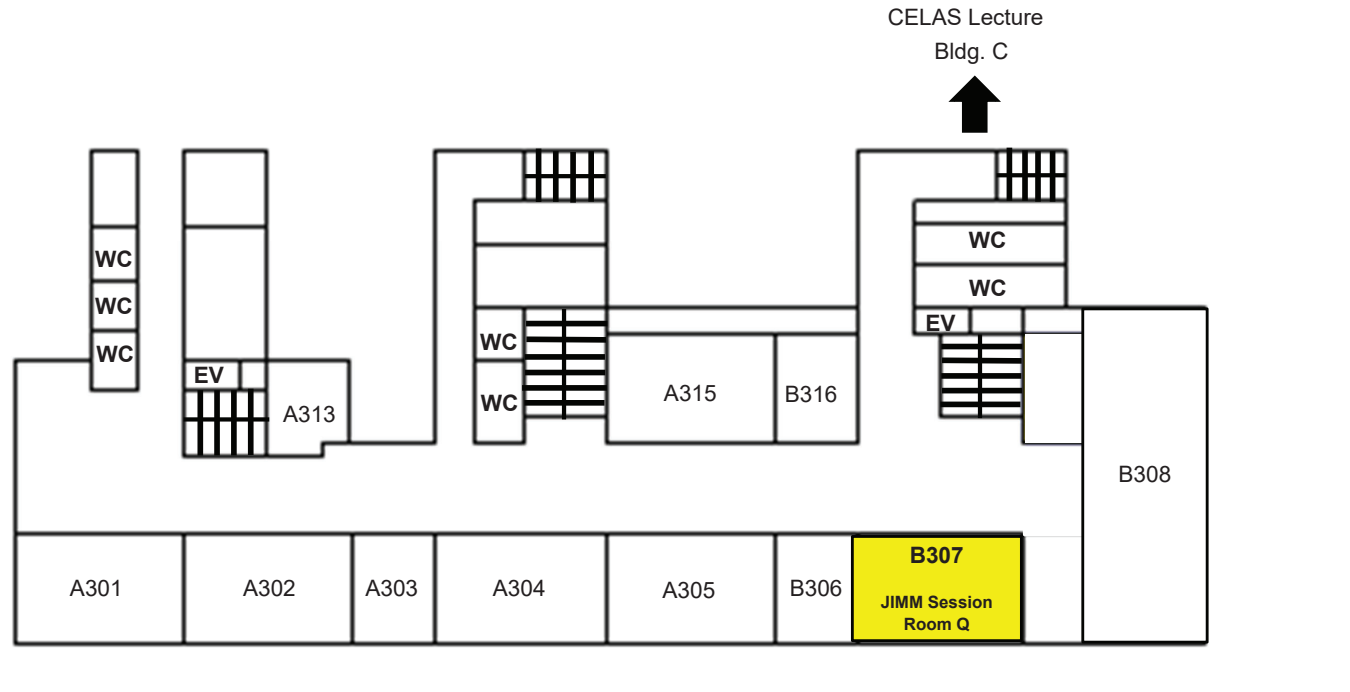

Osaka University Hall

1st Floor

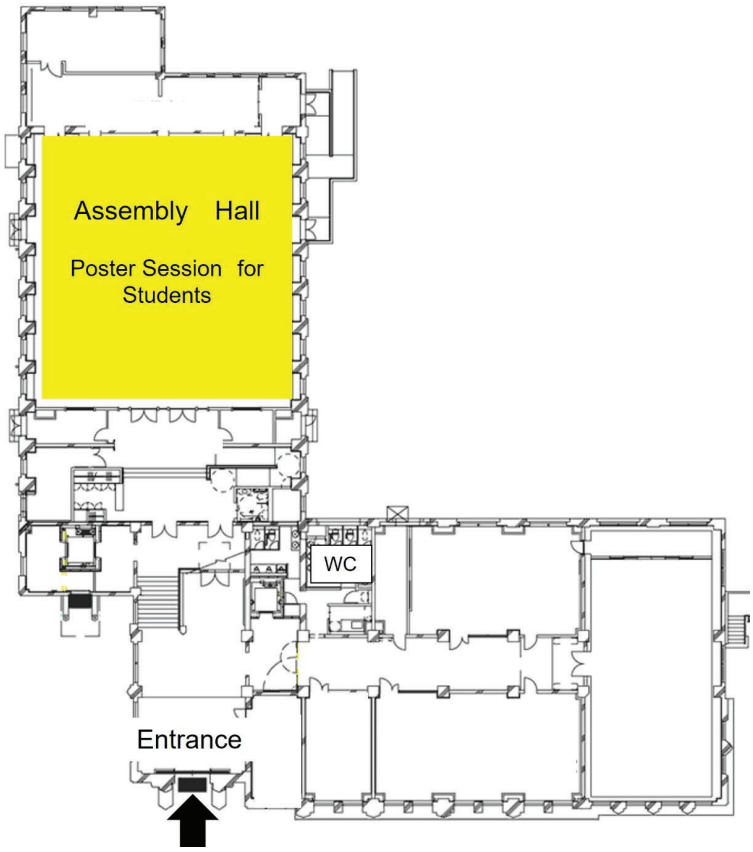

Science Commons

1st Floor

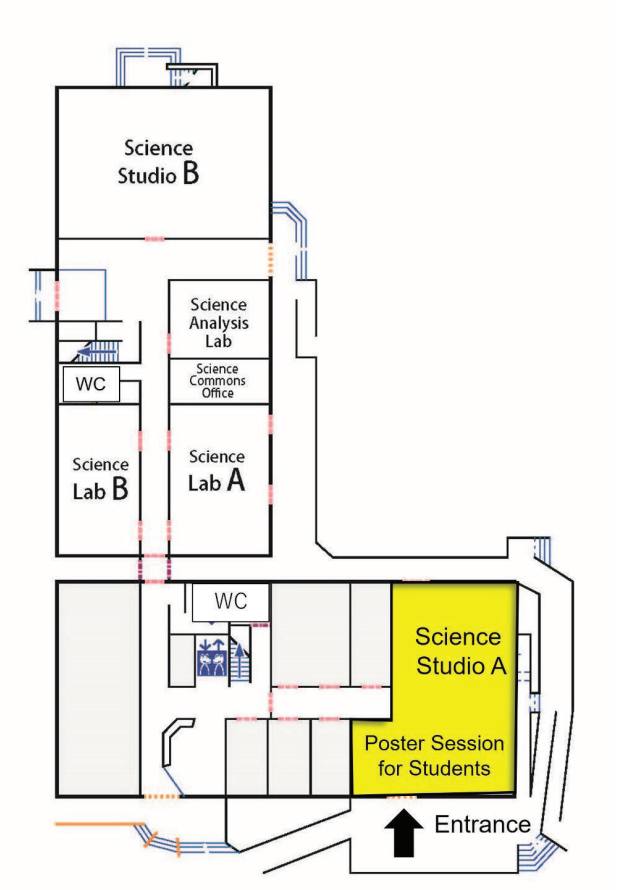

The timetable of the 188th ISIJ Meeting
(September 18-20, 2024 at Osaka University)

Session Room	Sept. 18 (Wed.)		Sept. 19 (Thu.)		Sept. 20 (Fri.)	
	AM	PM	AM	PM	AM	PM
Session Room 1 C401 CELAS Lecture Bldg. C	–	Fundamentals of solidification and continuous casting 1・2 [1–9] (13:00–16:20)	Introduction of research topics in novelprocessing forum 1・2 [35–40] (9:20–11:40)	Quantification of solidification phenomena V–1・2・3 [41–51] (13:00–17:10)	–	–
Session Room 2 C402 CELAS Lecture Bldg. C	Blast furnace / Evaluation of sinter reducibility [10–16] (9:00–11:40)	Young engineer session of ironmaking / New ironmaking [17–25] (13:00–16:20)	Microstructures and properties of iron ore sinters [Int.–1–Int.–6] (9:00–12:00)	Multi–scale evaluations on microstructures of high–quality iron ore sinters [D1–D4] (14:00–17:00)	Dephosphorization of iron ore / Sinter [74–79,111] (9:20–12:00)	–
Session Room 3 C406 CELAS Lecture Bldg. C	Frontiers of research on thermophysical properties and thermodynamics of high–temperature materials 1 [26–30] (9:20–11:00)	Frontiers of research on thermophysical properties and thermodynamics of high–temperature materials 2 [31–34] (13:00–14:20)	Inclusion 1・2 [52–58] (9:00–11:40)	Thermodynamics / Transport phenomena [59–65] (14:30–17:10)	–	–
Session Room 4 C301 CELAS Lecture Bldg. C	Cutting–edge of green technologies for carbon neutral of steelmaking industry 1・2 [88–93] (9:30–11:40)	–	Technology and culture of iron in Kinki region (10:00–17:30) [2,000yen, Student 1,000yen]		Development of green technology in surface treatment for high performance and corrosion resistance of steels (9:30–12:00) [Charge–Free]	–
Session Room 5 C302 CELAS Lecture Bldg. C	Final report of ISIJ innovative program for advanced technology "Sustainable clean Cr steel production process" (9:00–11:30) [Charge–Free]	Realization and challenges of building a sustainable society through utilization of iron and steel slag [Int.–7–Int.–16] (13:00–17:30)	Young engineer session of coke–making 1・2 [66–73] (9:00–12:00)	Risk assessment for steel supply chains (13:00–16:00) [Charge–Free]	Slag / Recycling of waste [80–87] (9:00–12:00)	Utilization of steel production by–product [94–98] (13:00–14:40)
Session Room 6 C306 CELAS Lecture Bldg. C	–	Characterization of steel–related materials using interdisciplinary methods 1・2 [210–218] (13:30–16:50)	Elemental analysis, Precipitate and inclusion analysis / Crystal structure analysis [219–225] (9:15–11:50)	Systems technologies toward enhancing energy efficiency [D5–D10] (13:30–17:10)	Instrumentation / Control and system [99–105] (9:00–11:40)	Current state and challenges for future advancement of instrumentation technology for iron making process Part 3 (13:00–16:00) [Charge–Free]
Session Room 7 C307 CELAS Lecture Bldg. C	Control technology for free cutting –16 / Lubrication and sintering [106–110, 112–113] (9:00–12:00)	Tribological studies on steel rolling [D11–D17] (13:00–17:00)	Research activity on the cooling model for the run–out table in the hot strip mill [D18–D26] (10:00–17:15)		Plating, Bar and wire / Modeling of various phenomena in metal forming and its application [114–120] (9:00–11:40)	Reliability of weld 6 / Hot rolling and oxide scale [121–128] (13:00–16:00)
Session Room 8 C308 CELAS Lecture Bldg. C	–	–	State–of–the–art research on material modeling [D27–D34] (9:00–17:00)		–	–
Session Room 9 C201 CELAS Lecture Bldg. C	Strength and deformation behavior 1・2 [129–136] (9:00–12:00)	Strength and deformation behavior 3 / Ductility and toughness [137–145] (13:00–16:20)	Stainless steels [167–169] (10:00–11:00)	Progress in development and reliability evaluation of structural materials supporting the liquefied hydrogen supply chain (13:00–17:00) [Charge–Free]	Strength and deformation behavior 4 / Fatigue [187–192] (9:30–11:50)	–
Session Room 10 C202 CELAS Lecture Bldg. C	Phase transformation and microstructure control [146–150] (10:00–11:40)	Recrystallization and growth・Modeling and simulation 1・2 [151–162] (13:00–17:30)	Heat resistant steels / Heat resistant alloys [170–175] (9:30–11:45)	The technical session by young engineers of hot rolling [176–180] (14:00–15:40)	Current status and issues for design of martensite and bainite in steels (9:00–16:20) [Charge–Free]	
Session Room 11 C203 CELAS Lecture Bldg. C	–	–	Approach of grain boundary engineering for achieving high–performance steels (10:00–17:00) [Charge–Free]		–	–
Session Room 12 C206 CELAS Lecture Bldg. C	Multi–phase structures and functionality in galvanized/aluminized coatings by hot–dip galvanizing process [D35–D40] (9:30–12:00)	Steels for machine structural use / Corrosion mechanism [163–166] (13:00–14:20)	Electrical steel / Soft magnetic material [181–186] (9:30–11:45)	Final report meeting of the "Study group on elucidation of microbiologically influenced corrosion and construction of diagnostic and countermeasure technologies (12:50–17:00) [Charge–Free]	–	–
Session Room 13 C102 CELAS Lecture Bldg. C	Innovative evaluation techniques for hydrogen entry and hydrogen trapping –IV [Int.–17–Int.–31] (9:00–17:05)		Roles of lattice defects in fracture and related characterization techniques: ductile fracture, metal fatigue, and hydrogen embrittlement (9:25–17:00) [Charge–Free]		Hydrogen embrittlement 1・2 [193–201] (8:40–12:00)	Hydrogen embrittlement 3・4 [202–209] (13:00–16:00)
JIMM Room C A102 CELAS Lecture Bldg. A	–	–	ISIJ and JIMM Joint Sessions Titan and its alloys 1・2 [J1–J8] (9:00–11:50)	ISIJ and JIMM Joint Sessions Titan and its alloys 3・4・5 [J9–J22] (13:00–18:00)	–	–
JIMM Room Q B307 CELAS Lecture Bldg. B	ISIJ and JIMM Joint Sessions Materials science of martensitic and bainitic transformations and its applications 1 [J23–J26] (10:30–11:50)	ISIJ and JIMM Joint Sessions Materials science of martensitic and bainitic transformations and its applications 2・3 [J27–J34] (13:00–15:55)	ISIJ and JIMM Joint Sessions Materials science of martensitic and bainitic transformations and its applications 4・5 [J35–J42] (9:00–11:50)	ISIJ and JIMM Joint Sessions Materials science of martensitic and bainitic transformations and its applications 6・7 [J43–J49] (13:00–15:35)		
	Banquet (18:30–20:30 at Senri Hankyu Hotel) (Toyonaka–city, Osaka) [12,000yen]		Poster Session for Students (11:00–14:00 at Osaka University Hall/ Science Commons) [Charge–Free] ISIJ Beer Party (17:30–19:00 at Toyonaka Fukuri Kaikan, 4Fl. Cafeteria) [1,000yen]		–	–

[ ]: Lecture Number
( ): Lecture Time
: Event to be held during the 188th ISIJ Meeting (Symposium, Poster Session for students)

Program of the 188th ISIJ Meeting (September 18-20, 2024)

Discussion Sessions

High Temperature Processes

Lecture No. / Discussion Session	Title	Speaker	Page
Multi-scale evaluations on microstructures of high-quality iron ore sinters			
D1	Effect of increment in Al_2O_3 concentration on microstructures of iron ore sinters from the perspective of the CaO-SiO_2-Fe_2O_3-Al_2O_3 system	M. Hayashi	299
D2	Evaluation of reducibility on multi-component calcium ferrite separated from iron ore sinter	D. Maruoka	303
D3	(ISIJ Research Promotion Grant) Observation of reduction reactions of iron-ore sinters using X-ray microscopes and prediction of reaction locations (“trigger sites”) by persistent homology	M. Kimura	305
D4	Crystal structure of SFCA phases in sintered ores: discovery of Fe_2O_3-rich SFCA-III phase	K. Sugiyama	309

Instrumentation, Control and System Engineering

Systems technologies toward enhancing energy efficiency			
D5	Toward systemic optimization of steel-making energy chains	H. Suwa	311
D6	Development of guidance system for fuel and power management in steel works	K. Suzuki	313
D7	Development of human cooperative simulator for fuel logistics planning at thermal power plants	T. Imoto	317
D8	A study on systemic optimization in steelworks responding to fluctuations in energy supply and demand	N. Fujii	321
D9	LCA research in the iron and steel industry and the possibility of applying systems approach	T. Nonaka	323
D10	Visualization of the lower steelmaking processes by time automata modeling	K. Sakakibara	325

Processing for Quality Products

Tribological studies on steel rolling			
D11	(Keynote Lecture) History of micro-plasto hydrodynamic lubrication in metal forming	A. Azushima	327
D12	Micro-plasto hydrodynamic lubrication in cold rolling of steel sheet (Influence of the surface roughness of steel sheet and roll)	T. Nishimura	331
D13	Discussion on micro-plast hydrodynamic lubrication in rolling based on *in situ* observation	H. Utsunomiya	335
D14	Measurement of oil film thickness distribution in roll-bite during cold rolling using quantum dots	M. Shimura	337
D15	Effect of plate surface condition and backward tension on lubricating behavior in cold rolling	A. Yanagida	339
D16	Development of stress distribution measurement method on roll surface during rolling	Y. Maeda	342
D17	3D FEM of temper rolling for investigation of roll deformation and friction	W. Baba	346
Research activity on the cooling model for the run-out table in the hot strip mill			
D18	Experimental study of rapid cooling technology	Y. Serizawa	349
D19	Construction of heat treatment analysis model considering transformation plasticity and accuracy verification	T. Fujisawa	350
D20	Model identification for coiling temperature control by optimization method	H. Imanari	354
D21	Spray cooling of high-temperature surfaces under controlled environmental conditions	M. Kohno	358
D22	Evaluation method of surface heat flux in water jet impingement on a moving hot body based on exact solution of heat conduction equation	T. Yamamoto	361
D23	Observation of morphology of voids in oxide scale formed on steel plate and evaluation of its effect on cooling	K. Kuwahara	362
D24	Revised method on inverse heat conduction and boiling heat transfer characteristics in spray cooling system with surface oxide film	N. Nagai	364
D25	Progress in an experimental study on laminar cooling heat transfer characteristics of ROT with hot rotating hollow cylinder quenching tests	Y. Mitsutake	366
D26	Characteristics of quenching sphere covered with thin film of Teflon into LN2	M. Monde	370
State-of-the-art research on material modeling			
D27	Proposal and applications of a ductile damage model accounting for anisotropy	K. Hayakawa	374
D28	Affordable measurement methods for yield surface of sheet metal (Simplified identification method using circumscribing polygon and rope-driven biaxial tensile method)	H. Takizawa	376
D29	Plastic flow rule in polycrystalline metal subjected to nonlinear loading paths	K. Yoshida	380
D30	(Invited Lecture) Crystal plasticity analysis of the differential hardening behavior under proportional loading path of a steel sheet	Y. Tsunemi	384

D31 Crystal plasticity modeling of ferrite-martensite dual phase steel sheets and predictions of their work-hardening behaviors under different loading paths — T. Hama · · · 386
D32 Texture and plastic deformation simulation in steels based on computational materials science — N. Fujita · · · 387
D33 Development of stretch flange crack prediction model considering crack form and strain gradient — Y. Maeda · · · 390
D34 (Invited Lecture) Modeling of sheet metal forming and fracture using Bayesian data assimilation — A. Yamanaka · · · 394

Microstructure and Properties of Materials

Multi-phase structures and functionality in galvanized/aluminized coatings by hot-dip galvanizing process

D35 Effect of alloy elements in steel sheets on solid-liquid interfacial reactions during hot-dipping in Zn-55%Al alloy melt — Y. Omi · · · 395
D36 Formation of intermetallic compounds in the initial stage of the interfacial reaction between αFe and liquid Zn at 450°C — I. Ohnuma · · · 398
D37 Dendrite growth direction and solidification path in Zn-Al system determined by X-ray imaging and diffraction — H. Yasuda · · · 399
D38 Reduction behavior of oxidized Fe-1Si alloy and oxygen emission behavior during reduction — Y. Tagaki · · · 403
D39 Elucidation of the kink band formation mechanism in Zn, investigated using single crystals and polycrystals — K. Hagihara · · · 405
D40 Effect of Multifunction Cavitation on fatigue properties of galvanized steel — H. Inoue · · · 409

Program of the 188th ISIJ Meeting (September 18-20, 2024)

International Organized Sessions

2024/9/19 Room 2

Lecture No. Title Speaker Page

Microstructures and properties of iron ore sinters

Session Organizers: M. Hayashi [Tokyo Inst. of Tech.], R. Murao [Nippon Steel]

9:00-9:05
Opening Address: M. Hayashi [Tokyo Inst. of Tech.]

Chair: R. Murao [Nippon Steel]

9:05-9:35
Int.-1 (Invited Lecture) Experimental study and thermodynamic modelling of the CaO-FeO-Fe_2O_3-Al_2O_3 system
Univ. of Queensland ○M. Shevchenko・H. Abdeyazdan・E. Jak, BHP S. Cheng ・・・ 413

9:35-10:00
Int.-2 Direct observation of melting behavior in iron ore mixture by synchrotron radiation X-rays
JFE ○K. Takehara・K. Ikeda・S. Morita, Kyoto Univ. T. Narumi・H. Yasuda ・・・ 416

10:00-10:25
Int.-3 Investigation of the gangue dissolution behavior into calcium ferrite in sinter using mineral liberation analysis
Kobe Steel ○T. Adachi・S. Yamazaki・K. Koga・K. Miyagawa ・・・ 418

Chair: K. Takehara [JFE]

10:35-11:05
Int.-4 (Invited Lecture) Development of predictive modeling of sinter productivity and strength using properties and microstructure of iron ores
POSCO ○M. Wang・J. Jeon ・・・ 420

11:05-11:30
Int.-5 (ISIJ Research Promotion Grant) Heterogeneous Fe chemical state evolution of iron ore sinters investigated by X-ray imaging and microanalysis
Osaka Univ. ○Y. Takeichi・Y. Ito, KEK Y. Niwa・M. Kimura ・・・ 422

11:30-11:55
Int.-6 Kinetic analysis on H_2-CO reduction of sintered Fe_2O_3-CaO-SiO_2-Al_2O_3 tablets at softening and melting temperature
Univ. of Toyama ○K. Kato・S. Yaguchi, National Inst. of Technology, Suzuka College H. Konishi, Univ. of Toyama H. Ono ・・・ 425

11:55-12:00
Closing Address: M. Hayashi [Tokyo Inst. of Tech.]

2024/9/18 Room 5

Lecture No. Title Speaker Page

Realization and challenges of building a sustainable society through utilization of iron and steel slag

Session Organizers: H. Matsuura [The Univ. of Tokyo], Y. Uchida [Nippon Inst. Tech.]

13:00-13:05
Opening Address: H. Matsuura [The Univ. of Tokyo]

Chairs: H. Matsuura [The Univ. of Tokyo], J. Nakano [MatterGreen]

13:05-13:30
Int.-7 (Keynote Lecture) Recent production, application and research activities for iron and steel slag in Japan
Nippon Inst. of Tech. ○Y. Uchida ・・・ 428

13:30-14:00
Int.-8 (Invited Lecture) Hot-stage slag engineering and downstream processing to deliver market-ready, sustainable products
KU Leuven ○Y. Pontikes・T. Hertel・M. Giels・R. E. Murillo Alarcón・G. Beersaerts ・・・ 431

14:00-14:30
Int.-9 (Invited Lecture) Research and application of high-grade asphalt pavement materials prepared from steel slag
Central Research Institute of China Baowu Iron and Steel Group ○Y. Xiao・Y. Li ・・・ 432

14:30-14:50
Int.-10 High-temperature carbonation of steelmaking slag
JFE ○M. Hiyoshi・H. Sugihara・N. Shigaki・J. Ishii・A. Murao ・・・ 436

14:50-15:10
Int.-11 Technology for production of calcium carbonate particles from steelmaking slag using glycerol solution for carbon dioxide fixation
Kobe Steel ○T. Sasaki・K. Sakai, Nihon Univ. T. Toyama ・・・ 437

Chairs: Y. Uchida [Nippon Inst. of Tech.], Y. Pontikes [KU Leuven]

15:25-15:55
Int.-12 (Invited Lecture) Contribution to building a sustainable society and carbon neutral in agriculture and marine through slag utilization
POSCO Environmental Planning Office ○H. Pak・M. Kim・J. Kim・C. Lee ・・・ 439

15:55-16:25
Int.-13 (Invited Lecture) The availability of valuable elements in various industrial slag/ash and their extraction/removal in support for the clean energy transition
MatterGreen ○J. Nakano ・・・ 440

16:25-16:45
Int.-14 Dissolution behavior of steelmaking slag fertilizer in soil
Nippon Steel ○S. Koizumi, Tohoku Univ. T. Iwama・M. Obara・S. Ueda ・・・ 442

16:45-17:05
Int.-15 Factors affecting microscopic basicity of silicate slags from the perspective of O1s binding energy -Toward strength prediction of blast furnace cement
Tokyo Inst. of Tech. ○M. Tsuji・T. Watanabe・M. Susa・M. Hayashi ・・・ 446

17:05-17:25
Int.-16 The utilization of metallurgical slag as ceramic materials
Inha Univ. ○Y. Kim, Korea Univ. J. Lee・S. Kim, Donga Univ. Y. Kang ・・・ 450

17:25-17:30
Closing Address: Y. Uchida [Nippon Inst. of Tech.]

2024/9/18 Room 13

Lecture No.
Title Speaker Page

Innovative evaluation techniques for hydrogen entry and hydrogen trapping -IV

Session Organizer: K. Fushimi [Hokkaido Univ.]

9:00-9:10
Opening Address: K. Fushimi [Hokkaido Univ.]

9:10-10:10
Int.-17 (Invited Lecture) Chances and challenges in hunting hydrogen
Johannes Kepler Univ. Linz ○A.W. Hassel ・・・ 452

Chair: Y. Sugawara [Shimane Univ.]

10:20-11:20
Int.-18 (Invited Lecture) Difference of C and N effect on hydrogen entry and diffusivity in austenitic stainless steels
POSTECH ○S.-J. Kim・K.-S. Kim, Yeungnam Univ. J.-H. Kang ・・・ 456

11:20-11:35
Int.-19 Effect of mechanical loading on the hydrogen diffusion behavior in tempered martensitic steel
Tohoku Univ. ○S. Ajito・H. Kakinuma, Tohoku Gakuin Univ. T. Hojo,
Tohoku Univ. M. Koyama・T. Hara, Nippon Steel T. Omura, Tohoku Univ. E. Akiyama ・・・ 460

11:35-11:50
Int.-20 Influences of lattice defect and crystal orientation on hydrogen diffusion in pure iron
Toyohashi Univ. of Tech. ○Y. Todaka・N. Adachi・Y. Abe・Y. Ishii・S. Wada・S. Kagawa ・・・ 461

Chair: A. Ooi [Tokyo Inst. Tech.]

13:00-14:00
Int.-21 (Invited Lecture) Scanning Kelvin probe techniques for mapping effective local hydrogen activity and permeation rates at lateral high resolution and sensitivity
Max-Planck-Institut fur Eisenforschung GmbH ○M. Rohwerder ・・・ 462

14:00-14:15
Int.-22 Visualization of hydrogen entry into high-strength steel during corrosion process using Mn oxide thin film
Shimane Univ. ○Y. Sugawara, JFE M. Omoda・S. Ootsuka ・・・ 464

14:15-14:30
Int.-23 Application of scanning blue-laser enhanced electrochemical microscope for evaluation of local hydrogen permeation rate of the steels
Kansai Univ. ○T. Haruna・K. Nogawa・T. Sakai・Y. Hirohata ・・・ 465

Chair: T. Igarashi [JAEA]

14:45-15:00
Int.-24 Spatially-resolved detection of hydrogen in steel by scanning photoelectron yield spectroscopy
Tohoku Univ. ○K. Miyamoto・T. Yoshinobu ・・・ 467

15:00-15:15
Int.-25 Effects of pH on local hydrogen entry behavior under NaCl droplet on Fe sheet
Tohoku Univ. ○H. Kakinuma・S. Ajito・M. Koyama・E. Akiyama ・・・ 468

15:15-15:30
Int.-26 Hydrogen permeation behavior of high strength steels with Laser activation
Hokkaido Univ. ○M. Sakairi・X. Han ・・・ 469

15:30-15:45
Int.-27 Effect of thiocyanate ion on hydrogen evolution reaction on steel
Tokyo Inst. of Tech. ○A. Ooi・A. Saito・E. Tada ・・・ 470

Chair: S. Ajito [Tohoku Univ.]

16:00-16:15
Int.-28 3D impedance measurement to investigate hydrogen evolution and permeation behavior on steel
Nagoya Inst. of Tech. ○Y. Hoshi・K. Tanaka ・・・ 471

16:15-16:30
Int.-29 In-situ quantitative evaluation of the hydrogen absorbed in steel plates and dependence of hydrogen content on specimen hardness
Hokkaido Univ. ○K. Fushimi・Y. Mizushiri・Y. Fujita・H. Habazaki ・・・ 472

16:30-16:45
Int.-30 Computational modeling for hydrogen entry into steel materials in acidic solutions containing chloride ions
NIMS ○H. Katayama・M. Kadowaki・M. Yamamoto ・・・ 474

16:45-17:00
Int.-31 Hydrogen absorption modeling using cellular automata
JAEA ○T. Igarashi ・・・ 475

17:00-17:05
Closing Address: K. Fushimi [Hokkaido Univ.]

Program of the 188th ISIJ Meeting (September 18-20, 2024)

High Temperature Processes

Lecture No. Plenary Session	Title	Speaker	Page
Fundamentals of solidification and continuous casting 1			
1	(ISIJ Research Promotion Grant) Evaluation of adhesion force acting on surface treated particles by water model experiment	H. Harada	477
2	Evaluation of flow conditions in tundish slag entrainment experiment	J. Nakashima	478
3	The recycle method of used Tundish refractory	Y. Nakamura	479
4	Effect of REM addition on fluctuation of mold bath level of ultra-low carbon steel	Y. Lu	480
5	Study on effect of addition of carbon by "Carbon Neutral" straw charcoal in mold flux	Y. Xu	481
Fundamentals of solidification and continuous casting 2			
6	Effect of Zr and Na on crystallization behaviors of cuspidine in mold fluxes	K. Mishima	482
7	Model experiments on the behavior of Ar gas injected into the molten steel flow from submerged entry nozzle	K. Fujita	483
8	Investigation of calculation for macro-segregation in 17-4PH stainless steel	S. Yano	484
9	Effect of Cu on the high temperature ductility of austenitic stainless steels	Y. Iwasaki	485
Blast furnace			
10	Influence of type of reducing agent injected into carbon recycling blast furnace on CO_2 emission amount	S. Uchida	486
11	Development of reverse engineering technology of the high-temperature reduction-softening phenomena of iron ore pellets bed using high-energy X-ray CT	S. Natsui	487
12	Development of blast furnace hot metal temperature estimation model	K. Ichikawa	488
13	Consideration of corrosion mechanism of main trough refractory by fluid analysis	N. Noguchi	489
Evaluation of sinter reducibility			
14	Reduction behavior of hematite- and goethite-based iron ore sinters	J. Ding	490
15	Quantitative method of mineral phase in iron ore sinter and reducibility evaluation	T. Murakami	491
16	Improvement of the evaluation method for sinter ore reducibility by X-ray CT method	T. Takayama	492
Young engineer session of ironmaking			
17	Stabilization measures of sinter quality at Kimitsu No.3 sinter plant	H. Eguchi	493
18	Development of degradation model for sinter ore considering reduction and particle size distribution	K. Nishihiro	494
19	Innovative ultra low carbon ironmaking technology with massive HBI charging in blast furnace	D. Hara	495
20	Factors inhibiting stable operation with low CR in Chiba No.6 blast furnace and their countermeasures	Y. Okamura	496
21	Improvement of blast furnace operation with cyber-physical system	R. Masuda	497
New ironmaking			
22	Effect of carbon morphology on melting behavior caused by carburization of vapor deposited carbon-iron oxide composite after reduction	R. Higashi	498
23	Low temperature reduction disintegration mechanism of self-fluxing pellet under hydrogen reduction shaft furnace	K. Momma	499
24	Effect of H_2-CO mixed gas reduction on the swelling behavior of iron ore pellets	K. Ohno	500
25	Direct iron ore reduction by hydrogen using plasma jet smelting	M. Uchikoshi	501
Frontiers of research on thermophysical properties and thermodynamics of high-temperature materials 1			
26	Clarification of the origin of excess volume in Fe-Pd alloys based on electronic states	M. Watanabe	502
27	(ISIJ Research Promotion Grant) Effect of cooling rate and aluminum addition on the structure of solidified calcium ferrite	S. Torige	503
28	Density and surface tension measurements of molten TiO_2, ZrO_2, and HfO_2 using pendant drop method	O. Takeda	504
29	Assignment of Raman signal related to local structure near Ti cation in silicate glasses	S. Sukenaga	505
30	Neural network analysis of viscosity of SiO_2-Al_2O_3-MgO-CaO-Na_2O melts	T. Sugawara	506
Frontiers of research on thermophysical properties and thermodynamics of high-temperature materials 2			
31	Effect of Al and S in molten steel on high temperature wettability of CaS	M. Ogawa	507
32	Comparison of surface tension for molten Fe-Si-Cu alloys: Measurements by electromagnetic levitation and predictions from the Butler model	M. Nishimura	508
33	Accurate evaluation of oxygen activity in surface tension measurements of molten metals using electromagnetic levitation	Y. Seimiya	509

34 Mixed modifier effect on thermal conductivity of CaO-MgO-$BO_{1.5}$-$AlO_{1.5}$ melts S. Yamada · · · 510

Introduction of research topics in novelprocessing forum 1

35 Microwave heating furnaces for industrial electrification and their scale-up research K. Kashimura · · · 511
36 Synthesis of carbon-based silicon carbide by multimode microwave irradiation J. Fukushima · · · 512
37 Suppression mechanism of β→γ transformation of $2CaO \cdot SiO_2$ S. Tashiro · · · 513

Introduction of research topics in novelprocessing forum 2

38 Infiltration behavior of molten metal into packed bed of alumina particles by ultrasonic irradiation K. Okumura · · · 514
39 Video analysis of solid particles alignment behavior induced by ultrasonic application to solid-liquid mixed phase Y. Miura · · · 515
40 Behavior of the anodized film formation under the imposition of intense magnetic field T. Kozuka · · · 516

Quantification of solidification phenomena V-1

41 Development of phase-field model explicitly solving sublattice composition T. Morino · · · 517
42 Quantitative evaluation of micro-segregation in Fe-C alloys by cellular automaton simulation K. Kaneko · · · 518
43 Three-dimensional simulations of simple shear deformation for semi-solid thin film utilizing multi-phase-field lattice Boltzmann model N. Yamanaka · · · 519
44 (ISIJ Research Promotion Grant) Construction of a multi-phase-field lattice Boltzmann model for three-dimensional multiple equiaxed dendrites settling in undercooled melt S. Sakane · · · 520

Quantification of solidification phenomena V-2

45 Model inclusion behavior near solid-liquid interface using cold model experiment Y. Miura · · · 521
46 Layered-structure solidification of peritectic reaction T. Horino · · · 522
47 Examination of crystallographic analysis method for massive-like transformation in carbon steel using 4D-CT+XRD M. Osaki · · · 523
48 Evaluating austenite grain coarsening following a massive-like ferrite-austenite transformation in Fe-0.45C steel using time-resolved X-ray diffraction Y. Wang · · · 524

Quantification of solidification phenomena V-3

49 Machine learning model for prediction of concentration distribution from optical micrograph M. Ohno · · · 525
50 Evaluating linear expansion coefficient and volume change due to phase transformation using 4D-CT+XRD T. Narumi · · · 526
51 Release of the NIMS thermodynamic database in python module format M. Ode · · · 527

Inclusion 1

52 Effect of oxides on characteristics of sulfides in Ca-treated resulfurized steel with different deoxidation modes Y. Li · · · 528
53 Three-dimensional characterization of MnS-Ti_2O_3 composite inclusions in steel by X-ray Micro-CT Z. Song · · · 529
54 Behavior of impurities and inclusions in stainless steel during arc melting under reduced pressure A. Yamada · · · 530

Inclusion 2

55 Influence of solidification rate on the inclusion evolution during unidirectional solidification of Fe-18Cr-2Mo alloy W. Xie · · · 531
56 Effect of deoxidation elements on sulfide inclusions in 16%Cr steel K. Matsuzawa · · · 532
57 Study on the floating behaviors of Al_2O_3 inclusion clusters in molten steel on basis of the three-dimensional quantitative characterization by X-ray Micro-CT T. Li · · · 533
58 Modification of alumina inclusions in molten steel by calcium treatment Y. Liu · · · 534

Thermodynamics

59 Thermodynamic evaluation on interaction coefficients of elements in molten iron K. Nagata · · · 535
60 Determination of interaction parameters of Al deoxidation of molten Fe-Ni alloy M. Iwabuchi · · · 536
61 Derivation of thermodynamic parameters between N and Mg in molten Fe by using Ag alloys K. Oshida · · · 537

Transport phenomena

62 Analysis of Cu-containing molten iron/molten slag interfacial electric properties during polarization by Electrochemical Impedance Spectroscopy S. Honna · · · 538
63 Evaluation of reduction rate of low-grade iron ore pellets with H_2 gas for direct hydrogen reduction S. Yaguchi · · · 539
64 Investigation of liquid slag properties using the aerodynamic levitation method under contactless conditions E. Cheremisina · · · 540
65 Phosphorus metal/slag distribution behavior in electric arc furnace melting of hydrogen direct reduction iron Y. Ito · · · 541

Young engineer session of coke-making 1

66 Gas Section operation influence and correspondence of the coke oven operation decreases — M. Yamamoto · · · 542
67 Optimization of wastewater treatment plant operation — Y. Higashi · · · 543
68 Replacement of coke oven front bricks — T. Mizukawa · · · 544
69 Estimation method of the amount of deposit carbon on coke oven wall — S. Okutani · · · 545

Young engineer session of coke-making 2

70 Position monitoring of coke oven trolley wire and current collector — A. Ogawa · · · 546
71 Upgrade construction of the large-scale COG duct in the gas purifying process — T. Koh · · · 547
72 Method for utilizing Non-Caking Coal with new coal-fluidity evaluation — S. Arakawa · · · 548
73 Quantification of coke gasification reaction region using X-ray CT and three-dimensional image analysis — H. Hayashizaki · · · 549

Dephosphorization of iron ore

74 Rate of volatilization removal of phosphorus for high phosphate iron ore by vacuum electrothermal reduction — E. Shibata · · · 550
75 Effect of iron ore mineral types on dephosphorization with reduction gasification (Developing dephosphorization technique for iron ore -1) — Y. Yamaguchi · · · 551
76 Properties of continuous dephosphorization for iron ore using rotery kiln type furnace (Developing dephosphorization technique for iron ore -2) — O. Ishiyama · · · 552

Sinter

77 Combustion behavior of coke in the presence of hematite-magnetite in quasi-particles — W. Kodama · · · 553
78 Effect of re-ignition on sinter microstructure at iron ore sintering process development of REMO-tec (RE-ignition method for optimization of total energy consumption)-9 — K. Hirano · · · 554
79 Reduction rate of nitrogen oxide by calcium ferrite compounds — S. Nagae · · · 555
111 Development of automatic iron ore sintering operation control technology using video AI technology — J. Park · · · 587

Slag

80 Development of technology to reduce deposits inside a torpedo car using mineral phase analysis — M. Iwasaki · · · 556
81 Measurement of the steam behavior of steelmaking slag steam aging — H. Yano · · · 557
82 Enrichment behavior of Sm in steelmaking slag — W. Gu · · · 558
83 Metal recovery from Electric arc furnace oxidizing slag by low temperature reduction — R. Kitagawa · · · 559
84 Mechanism of Inhibition for Cr Dissolution from Steelmaking Slag — T. Iwama · · · 560

Recycling of waste

85 Synthesis of $LiFePO_4$ using $FePO_4$ crystallized from steelmaking slag extract — J. Deng · · · 561
86 Analysis of temperature distribution in phosphoric acid reduction process — S. Ishihara · · · 562
87 Study on the comparison of various carbon materials on reduction reaction phosphoric acid to produce white phosphorus — A. Siahaan · · · 563

Sustainable Systems

Lecture No. / Plenary Session — Title — Speaker — Page

Cutting-edge of green technologies for carbon neutral of steelmaking industry 1

88 Fundamental research for isothermal regulation of CO_2 methanation reactor by catalyst with thermal energy storage function — K. Mimura · · · 564
89 Optimization and structural evaluation of Al-Cu-Si based latent heat storage particles for high-temperature waste heat recovery — M. Jeem · · · 565
90 Evaluation of the heat storage and release performance in a 300kWh scale packed bed system with medium to high-temperatures latent heat storage pellets using a numerical model — T. Nakamura · · · 566

Cutting-edge of green technologies for carbon neutral of steelmaking industry 2

91 Carbothermal reduction behavior of iron-based alkaline leaching process residue of EAF dust — D. Hidaka · · · 567
92 Formation of Fe_3C at low carbon activity — K. Ikeda · · · 568
93 Process engineering approach to low temperature carburization of high purity Iron (so-called Tamahagane) — Y. Matsui · · · 569

Utilization of steel production by-product

94 Analysis of phosphorus (P_4) formation reaction by gas analysis method — R. Iwahana · · · 570

95 Effect of slag carbonation on Fe dissolution behavior of steelmaking slag granules — M. Takano · · · 571
96 Development of alkaline leaching process of zinc from EAF dust (Part 2) — K. Haiki · · · 572
97 Separation of each and every element contained in blast-furnace slag by treating with citric acid aqueous solution — H. Sakane · · · 573
98 (ISIJ Research Promotion Grant) Absorption behavior of CO_2 to calcium citrate synthesized from blast furnace slag — K. Kubota · · · 574

Instrumentation, Control and System Engineering

Lecture No. / Plenary Session — Title — Speaker — Page

Instrumentation

99 Measurement of flank surface of threads for OCTG used focusing method — S. Oshima · · · 575
100 Comparison of measurement accuracy between the Rhodes method and the sampling moire method for measuring displacement of structures at long range — T. Sano · · · 576
101 Monitoring method of polygonal wear of rolls of rolling mills — K. Kawamura · · · 577

Control and system

102 Design method for optimal manufacturing conditions using a hybrid method of machine learning and optimization. — K. Uchino · · · 578
103 Development of analysis system for through-process material quality data — H. Takagi · · · 579
104 Overfitting control in nodel training using data augmentation and overfitting judgement based on prediction values — Y. Seki · · · 580
105 A data-driven state feedback design for LQ regulator — Y. Fujisaki · · · 581

Processing for Quality Products

Lecture No. / Plenary Session — Title — Speaker — Page

Control technology for free cutting -16

106 Fundamental study on machinability of scale with S55C-Effect of scale on tool wear- — M. Hagino · · · 582
107 Measurement of temperature on rake face of tool during cutting of heat treated carbon steel — A. Ikuta · · · 583
108 Influence of polymer addition cutting fluid on machinability of S55C steel — A. Takemura · · · 584
109 Spallation resistance of coated cemented carbide with shot-peening — M. Okada · · · 585

Lubrication and sintering

110 3D analysis of the periodicity of pore distribution in Ti L-PBF material — R. Yoshida · · · 586
112 Development of water-soluble belt grinding oil for stainless steel — N. Tanino · · · 588
113 Micro-plasto hydrodynamic lubrication in cold rolling of steel sheet 4 (Influence of viscosity of lubricant) — T. Nishimura · · · 589

Plating, Bar and wire

114 Effect of coating composition on the corrosion resistance of Zn-based plated steel sheets in soil — A. Shimizu · · · 590
115 The influence of dynamic wetting on hot dip galvanizing — C. Jee · · · 591
116 Cause of bending fracture in high-strength fasteners and heredity of surface recarburization in high carbon steel — T. Zhang · · · 592

Modeling of various phenomena in metal forming and its application

117 Evaluation of damage threshold value of an anisotropic damage model — K. Hayakawa · · · 593
118 Collision behavior of various metal sheets in magnetic pulse seam welding — M. Miyazaki · · · 594
119 Effect of oxide layer fracture on the cold-forge solid phase welding — N. Yukawa · · · 595
120 Height dependencd of large-Scale void closure behavior during hot rolling — N. Ueshima · · · 596

Reliability of weld 6

121 Correlation between microstructure and toughness in high current buried arc weld metal — F. Tanaka · · · 597
122 (ISIJ Research Promotion Grant) Dissimilar welding of steel to aluminum alloy via solid-state welding using local resistance heating — Y. Sato · · · 598
123 Prediction of weld solidification cracking susceptibility of dissimilar welds using austenitic metals — K. Kadoi · · · 599
124 Numerical simulation of flux-wall guided transfer in submerged arc welding by particle method — H. Komen · · · 600
125 Numerical simulation of TIG welding with electromagnetic controlled molten pool method — Y. Kobayashi · · · 601

Hot rolling and oxide scale

126 Effect of Sn on Cu intergranular penetration at temperatures lower than the melting point of Cu — Y. Kohigashi · · · 602
127 Surface cracking due to hot shortness in hot rolling of Cu bearing steel. — N. Tsuchida · · · 603
128 Microstructure revelation of oxide scale on hot rolling steels and its phase transformations — I. Sohn · · · 604

Microstructure and Properties of Materials

Lecture No. / Plenary Session — Title — Speaker — Page

Strength and deformation behavior 1

129 Crystal plasticity analysis of strain localization in quenching and partitioning steel — W. Yin · · · 605
130 Heterogeneous deformation within local deformation bands in ultra-low carbon ferritic steel — Y. Sato · · · 606
131 Work-hardening rate in Fe-Al alloys measured using a microcantilever method — S. Inoue · · · 607

Strength and deformation behavior 2

132 Relationship between local deformability and tempering temperature in martensitic steels — T. Yoshii · · · 608
133 Effect of MnS inclusion on deformation behavior of martensitic steel under bending — T. Otsuki · · · 609
134 Dislocation characteristics and work hardening behavior in lath martensite transformed from deformed austenite — T. Osanai · · · 610
135 Suppression of surface fatigue crack initiation by selective local work hardening at the potential crack initiation site using pre-fatigue deformation in 1.6 GPa martensitic steel — K. Okada · · · 611
136 Visualization of strain distribution around fatigue crack introduced by cyclic bending of SUS301 steel — N. Koga · · · 612

Strength and deformation behavior 3

137 Observation of dislocations around plate-shaped VC after pre-straining — E. Shimoda · · · 613
138 Analysis of tensile properties in dual phase steel with controlled ferrite phase — K. Ogatsu · · · 614
139 Effect of thermomechanical treatment on tensile properties of TRIP-aided steel sheet with bainitic ferrite and martensite — S. Fukasaku · · · 615
140 Effect of retained austenite on warm tensile properties of warm-rolled TBM steel — K. Hattori · · · 616
141 Development of high elongation type of 780MPa TRIP steel with excellent properties for automotive applications — K. Jung · · · 617

Ductility and toughness

142 Effects of P and S on low temperature toughness of tempered martensite in low alloy steel — H. Ogawa · · · 618
143 Multistage fracture generation factors in fracture toughness tests of high-Ni steels — Y. Hasegawa · · · 619
144 Effect of intergranular carbide on tensile properties in high-strength high-toughness hypereutectoid-steels — N. Harada · · · 620
145 Brittle fracture mechanism in fully pearlitic steel — K. Hyodo · · · 621

Phase transformation and microstructure control

146 Competitive formation of acicular and globular austenite during reverse transformation from martensite in Fe-0.18C-8Mn alloy — L. Fan · · · 622
147 Mn enrichment into cementite during pearlitic transformation and subsequent isothermal holding in Fe-C-Mn Alloy — K. Fujikura · · · 623
148 Interfacial segregation / partitioning of Mn and energy dissipation during ferrite growth in decarburized Fe-C-Mn alloy — K. Sato · · · 624
149 Control of ferrite morphology in austenitic stainless steel weld metal solidified with primary ferrite — K. Kadoi · · · 625
150 3D in situ analysis for deformation-induced martensitic transformation in austenitic steel by synchrotron X-ray — T. Iwano · · · 626

Recrystallization and growth

151 Contentious recrystallization of ferrite in pearlite initial microstructure — N. Nakada · · · 627
152 Effect of Nb and Sb addition on recrystallization during annealing in high strength steel sheet — R. Morimoto · · · 628
153 Development of scanning X-ray orientation laminography — Y. Hayashi · · · 629
154 Cellular automaton simulation on cellular grain growth in solid phase (Influence of temperature gradient, heat source scanning, and prioritized grain growth) — Y. Adachi · · · 630

Modeling and simulation 1

155 Optimization of heat treatment conditions in tempered martensite steel by machine learning — K. Sawai · · · 631
156 Development of prediction model for material properties of spring steels by machine learning — K. Takahashi · · · 632

157 Deep learning approaches for establishing the heat treatment condition-microstructure-property relationship — H. Kim · · · 633
158 Prediction of residual stress in additively manufactured 18Ni300 maraging steel using GAN-based deep learning method — K. Seyun · · · 634

Modeling and simulation 2

159 (ISIJ Research Promotion Grant) A finite element simulation of rate and size dependences of strain-induced martensite transformation by thermo-coupled crystal plasticity based on microforce — Y. Huang · · · 635
160 Inverse estimation of parameters in 3D phase-field model for γ → α transformation in steel — K. Nakayama · · · 636
161 Feature extraction using three-dimensional variational auto-encoder for austenite-to-ferrite transformation behavior in pure iron — M. Serada · · · 637
162 Topological features of ferrite grain boundary structure and its connections with C segregation — Y. Zhang · · · 638

Steels for machine structural use / Corrosion mechanism

163 Behavior of high temperature nitriding on low carbon low alloy steel — R. Takao · · · 639
164 Role of hardness distribution on pitting strength for nitrided-SCM440H steel — T. Maruyama · · · 640
165 Effect of oxygen concentration on salt spray test — K. Sugimoto · · · 641
166 Based on thermomechanical process, Development of non-heat treated CHQ products — J.-S. Lee · · · 642

Stainless steels

167 Dislocation density within each phase of a hot worked duplex stainless steel — M. Kawa · · · 643
168 Effects of cooling rate and composition on the structure of SUS430 cooled from (α+γ) phase — T. Mizoguchi · · · 644
169 Development of high-strength stainless steel 316LH for liquefied hydrogen — S. Song · · · 645

Heat resistant steels

170 Effect of boron addition on creep strength and precipitates of UNS S31740 — N. Otaki · · · 646
171 Precipitation behavior of $M_{23}C_6$ phase on the coherent twin boundary of KA-SUS310J1TB during aging — T. Hatakeyama · · · 647
172 Grain boundary engineering of KA-SUS310J1TB — S. Sekine · · · 648

Heat resistant alloys

173 (ISIJ Research Promotion Grant) Evaluation of grain boundary and interphase boundary strength in Ni–Cr binary alloy with nanoindentation method — R. Nagashima · · · 649
174 Effects of substitution of Ta by V on microstructure evolution in alloy Ta-718 — S. Nishida · · · 650
175 Measurement of dislocation density and twin density by X-ray diffraction in-situ tensile test at elevated temperature in the SLM fabricated Inconel738LC superalloy — A. Ito · · · 651

The technical session by young engineers of hot rolling

176 Development of feed forward control based on sheet bar camber — K. Komiya · · · 652
177 Increase in calorific value of MIX gas for improvement of energy conservation — N. Kajii · · · 653
178 Countermeasure for the excessive temperature increase on slab's longitudinal edge in reheating furnace — K. Oki · · · 654
179 Improvement of fuel intensity by developing thermal insulation of heating furnace and reduction of meandering of slab in-furnace — A. Nakamura · · · 655
180 Prevention of generation of creases in low-carbon steel sheets — S. Akiyama · · · 656

Electrical steel

181 Deformation structure and texture of 3% Si steel with coarse {100}<001> grains — T. Murakawa · · · 657
182 Texture evaluation of heavily cold-rolled 3% Si steel using spherical indexing of EBSD pattern — M. Takenaka · · · 658
183 Active slip systems and crystal rotation during simple shear deformation of Fe-3%Si — N. Wada · · · 659

Soft magnetic material

184 Effect of warm rolling reduction rate on microstructure, Texture and magnetic properties of Fe-18Co-xSi-0.5Al mass% alloys — T. Sato · · · 660
185 Relationship between composition, chemical bonding state, and magnetostriction in amorphous Fe-B-N alloy flim — N. Isogai · · · 661
186 Effect of nitrogen addition on the magnetostrictive coefficients of soft magnetic Fe-Al alloy single-crystal films — K. Imamura · · · 662

Strength and deformation behavior 4

187 Effects of annealing on microstructure and mechanical properties in Fe-Ni-Al-C alloys — K. Takahata · · · 663
188 Effect of γ-phase stability and second phase volume fraction on tensile properties of Fe-Ni-Al-C alloys — K. Kimura · · · 664

189 (ISIJ Research Promotion Grant) Achieving remarkable enhancement of yield strength ensuring large ductility in a metastable $Fe_{50}Mn_{30}Cr_{10}Co_{10}$ high-entropy alloy via warm rolling treatment — X. Lan · · · 665

Fatigue

190 (ISIJ Research Promotion Grant) Development of solid carburizing process with innovative mechanisms (Evaluation of fatigue properties) — T. Aoki · · · 666

191 Fatigue properties of linear friction welded low carbon steel cruciform joints — H. Miao · · · 667

192 (ISIJ Research Promotion Grant) Static fatigue behavior of Cr_2O_3 in atmosphere containing water vapor at high temperatures — K. Yen-Ling · · · 668

Hydrogen embrittlement 1

193 Thermally activated dislocation motion in H-charged Fe-Cr-Ni austenitic steel: a study via room temperature creep — Y. Ogawa · · · 669

194 Stacking fault probabilities in hydrogen-charged SUS310S steel during low temperature deformation — T. Ito · · · 670

195 Hydrogen-induced strain localization phenomena in an austenitic FeMnAlC low-density steel — I. Gutierrez · · · 671

196 In-situ 0.3mm thin wall hollow high pressure hydrogen low temperature tensile test with X-ray diffraction using Synchrotron radiation, Tansformation behavior — S. Torizuka · · · 672

197 (ISIJ Research Promotion Grant) Formation process of hydrogen-induced vacancies in austenitic stainless steel SUS 304 by positron annihilation lifetime spectroscopy — L. Chiari · · · 673

Hydrogen embrittlement 2

198 Effect of carbide morphology on hydrogen-related fracture behavior in tempered martensitic steels — E. Nakagawa · · · 674

199 Relationship between hydrogen embrittlement susceptibility and local stress / strain concentration in low-carbon martensitic steel — K. Okada · · · 675

200 Main factors of hydrogen-related intergranular and transgranular fractures in elastic and plastic regions of tempered martensitic steel — K. Okuno · · · 676

201 Comparison of hydrogen embrittlement fractures of tempered martensitic steel obtained by various test methods — R. Tokizaki · · · 677

Hydrogen embrittlement 3

202 Strain-controlled low-cycle fatigue testing for pipeline steel X65 under cathodic hydrogen charging — T. Homma · · · 678

203 Evaluation of the activation energy of hydrogen desorbed from the vicinity of dislocation cores in iron — K. Akiyama · · · 679

204 (ISIJ Research Promotion Grant) Evaluation of hydrogen atoms trapped at vacancies in α-iron using rate theory — K. Sato · · · 680

205 Carbide precipitation and hydrogen trapping behavior in Mo and Ti added tempered martensitic steel — M. Kameya · · · 681

Hydrogen embrittlement 4

206 First-principles study of grain boundary segregation at prior γ grain boundaries for suppression of hydrogen embrittlement — K. Ito · · · 682

207 Prediction of the effect of alloy element addition on the cohesive energy of prior γ grain boundaries for suppression of hydrogen embrittlement — K. Ito · · · 683

208 Quantitative estimation method for segregated solute effects on hydrogen-enhanced decohesion at a grain boundary — M. Yamaguchi · · · 684

209 The effect of alloying element on hydrogen solubility of Fe-Cr-Ni alloys: First-principles calculation of the anergy effect of Cr, Ni atoms on hydrogen absorption energy — J. Moriyama · · · 685

Process Evaluation and Material Characterization

Lecture No. / Plenary Session — Title — Speaker — Page

Characterization of steel-related materials using interdisciplinary methods 1

210 Stability of oxidation state of iron in organic acid complex — M. Uchikoshi · · · 686

211 Characterization of residual stress and microstructure in multi-component iron alloys — S. Suzuki · · · 687

212 Mechanism of cathodoluminescence for internal α-alumina on heat-resistant alloy — S. Imashuku · · · 688

213 Observation of dislocation multiplication during tensile/compressive deformation using in-situ neutron diffraction — S. Karasawa · · · 689

214 Characteristics of structure and properties of glasses containing various oxyanions — S. Suzuki · · · 690

Characterization of steel-related materials using interdisciplinary methods 2

215 (ISIJ Research Promotion Grant) Relationship between work hardening behavior and dislocation structure in high nitrogen austenitic steel — T. Masumura · · · 691

216 The interaction between N-Cr pairs and dislocations in nitrogen-added austenitic stainless steels — Y. Kawahara · · · 692

217 Characterization of dislocation structures in austenitic stainless steels with different nitrogen content and deformation temperatures — H. Harako ・・・ 693

218 (ISIJ Research Promotion Grant) Development of operando positron annihilation lifetime spectroscopy for the H-related vacancies in iron — M. Fujinami ・・・ 694

Elemental analysis, Precipitate and inclusion analysis

219 (ISIJ Research Promotion Grant) 3D elemental analysis of reinforced concreate in salt water by confocal X-ray fluorescence measurements — T. Matsuyama ・・・ 695

220 Factors affecting accuracy and precision for gravimetric analysis of sulfur in steel — N. Uehara ・・・ 696

221 Determination of valence and local structure analysis of iron in melting slags by using the XAS technique — K. Shinoda ・・・ 697

222 Evaluation method for nonmetallic inclusions in large volume of steel materials utilizing hydrogen embrittlement — Y. Kobanawa ・・・ 698

Crystal structure analysis

223 (ISIJ Research Promotion Grant) Development of non-destructive imaging methods of bulk crystalline phase fraction by neutron transmission double Bragg-edges analysis — H. Sato ・・・ 699

224 Development of simultaneous analysis of stress and dislocation density for neutron Bragg-edge imaging — S. Kuromi ・・・ 700

225 Revaluation of a formula converting Bragg-edge width to Vickers hardness in wavelength-resolved neutron imaging — N. Murohashi ・・・ 701

ISIJ and JIMM Joint Sessions

Lecture No. Joint Session	Title	Speaker	Page
Titan and its alloys 1			
J1	Effect of nitrogen content on deformation and fracture behavior of Ti-N alloys	T. Katayama	702
J2	Effect of oxygen content on slip system activity in rolled pure titanium sheets	T. Hirooka	703
J3	Deformation under cyclic fatigue and dwell fatigue in high oxygen solid solution titanium	S. Hara	704
J4	Effect of oxygen addition on microstructure formed of furnace-cooled Ti-Fe-O alloys	I. Masumi	705
Titan and its alloys 2			
J5	High-temperature forging and plastic properties of aircraft Ti-17 alloy: Estimation of governing factors through experiments and machine learning	M. Kanamaru	706
J6	Unusual Hall-Petch relation of a Ti-6Al-2Sn-4Zr-2Mo-Si alloy with martensitic duplex (α+α") microstructure: effects of grain size and texture.	I. Sechepee	707
J7	Automatic detection of crystal grains in Ti-6Al-4V alloy and prediction of mechanical properties by machine learning	K. Sugio	708
J8	Grain boundary extraction of pure titanium using automatically generated images with different real-structure similarity	K. Ozaki	709
Titan and its alloys 3			
J9	The effect of strain rate on flow stress in commercial pure titanium sheet	H. Takebe	710
J10	Effect of alloying elements on creep behavior of α+β type titanium alloys at room temperature	S. Hashimoto	711
J11	The influence of alloying elements and microstructure control on the deformation behavior of the new Ti-6Al-5.5V-0.5Ni-0.5Cu alloy	Y. Kassai	712
J12	Solid-solution and precipitation strengthening effect on Ti-Zr-Al-Nb alloys	K. Kim	713
J13	Effect of Nb addition on microstructure with compositional modulation and mechanical properties of Ti–Zr alloys	N. Nagai	714
Titan and its alloys 4			
J14	canceled	X. Wang	
J15	Effect of Al content on microstrucutre and superelastic properties of metastable β-type Ti–Fe–Al alloys	N. Nohira	716
J16	Development of radiation damage-tolerant high-intensity proton accelerator beam window using Ti-15V-3Cr-3Al-3Sn Alloy (I)	T. Ishida	717
J17	Development of radiation damage-tolerant high-intensity proton accelerator beam window using Ti-15V-3Cr-3Al-3Sn alloy (ii)	K. Furuya	718
Titan and its alloys 5			
J18	Microstructures and mechanical properties of dissimilar linear friction welded Ti6246/Ti64 joint	N. Kinouchi	719
J19	Microstructure and room temperature tensile properties of layered Ti-Mo structure by hot rolling of stacked sheets	S. Emura	720
J20	Improvement of an open atmospheric nitrided titanium surface using an electric field assisted laser-induced plasma	A. Yoshino	721
J21	Characteristic control of an open atmospheric nitrided Ti layer through the adjustment of heat transfer from the laser-induced plasma	K. Yonemoto	722
J22	Manufacturing of metallic titanium from tip using thermal decomposition	N. Watanabe	723
Materials science of martensitic and bainitic transformations and its applications 1			
J23	Comprehensive understanding for rank-1 connection of habit plane variants	N. Takahashi	724
J24	Effect of external constraints on martensitic transformation in Fe-Ni alloy	T. Masukawa	725
J25	Evaluation of microscopic internal stresses in lath martensite by pinhole FIB-DIC	W. Zhao	726
J26	Prediction of transformation-induced internal stresses in martensitic steels by Eshelby's inclusion theory	K. Tamura	727
Materials science of martensitic and bainitic transformations and its applications 2			
J27	A mechanism for dependency of Ms on gain size of austenite III	T. Tomida	728
J28	Crystallographic analysis of stress-induced martensite in Ti-Ni alloy single crystal	K. Ono	729
J29	Crystal orientation dependence of stress-induced martensitic microstructure in single crystals of Ti-Mo-Al alloy	K. Izumi	730
J30	Effect of Mn content on critical stresses in single-crystal Cu-Al-Mn superelastic alloys	Y. Tanikawa	731

Materials science of martensitic and bainitic transformations and its applications 3

J31 Diffusion behavior in Cu-Al-Mn Superelastic alloy during low temperature heat treatment: XAS and DFT study — Z. Liang · · · 732

J32 Magnetic domain observations in polytwin microstructure of Fe-61.8at.%Pd — Y. Tomita · · · 733

J33 Analysis on reverse transformation behavior of 0.1C-2Si-5Mn steel by transmissyon X-ray diffraction at high temperature using Synchrotron radiation in SPring-8 — S. Torizuka · · · 734

J34 Effect of Mo addition on the toughness of 10%Mn-0.1%C steel at inter critical annealing — H. Kubota · · · 735

Materials science of martensitic and bainitic transformations and its applications 4

J35 Superelasticity in Fe-Mn-Al-Si alloys — K. Edagawa · · · 736

J36 Exploration of shape memory alloy in the Ti-Al-Cr system using diffusion couple and micro-Vickers techniques — Y. Song · · · 737

J37 Martensitic transformation and superelasticity in Ti-Al-V alloys — R. Hasegawa · · · 738

J38 (Keynote Lecture) The effect of B2 precipitates on lath martensite transformation behavior in Fe-Ni-Al alloys — G. Yokoo · · · 739

Materials science of martensitic and bainitic transformations and its applications 5

J39 Unveiling hierarchical phase transformations at ε-ε martensite intersections — D. Singh · · · 740

J40 Stabilization by prior deformation in metastable austenitic steel undergoing γ→ε→α' transformation — M. Otaki · · · 741

J41 Application of Ti-Ni-Nb alloy for active operative heat storage material — H. Nakayama · · · 742

J42 Metamagnetic transition of Mn_3Ga alloy with small hysteresis — D. Imatomi · · · 743

Materials science of martensitic and bainitic transformations and its applications 6

J43 Strengthening mechanism in as-quenched martensite [1] Dislocation strengthening in pure iron martensite — S. Takaki · · · 744

J44 Strengthening mechanism in as-quenched martensite [2] Dislocation strengthening in martensite containing carbon — Y. Hiyama · · · 745

J45 Plastic deformation mechanism of low-carbon steel lath martensite by multiscale deformation analysis — S. Gong · · · 746

J46 Deformation behavior of ultrafine-grained austenitic steel at low temperatures — S. Harjo · · · 747

Materials science of martensitic and bainitic transformations and its applications 7

J47 CNN-based image regression analysis for linking microstructure and property of tempered martensite — Y. Adachi · · · 748

J48 Phase-field analysis of martensite transformation in steel under continuous cooling condition — T. Okamoto · · · 749

J49 Effect of internal stress field on hydrogen diffusion in martensite microstructure in steel — A. Yoshida · · · 750